

Stringent test of CP symmetry in Σ^+ hyperon decays

M. Ablikim¹, M. N. Achasov^{4,c}, P. Adlarson⁷⁶, X. C. Ai⁸¹, R. Aliberti³⁵, A. Amoroso^{75A,75C}, Q. An^{72,58,a}, Y. Bai⁵⁷, O. Bakina³⁶, Y. Ban^{46,h}, H.-R. Bao⁶⁴, V. Batzskaya^{1,44}, K. Begzsuren³², N. Berger³⁵, M. Berlowski⁴⁴, M. Bertani^{28A}, D. Bettoni^{29A}, F. Bianchi^{75A,75C}, E. Bianco^{75A,75C}, A. Bortone^{75A,75C}, I. Boyko³⁶, R. A. Briere⁵, A. Brueggemann⁶⁹, H. Cai⁷⁷, M. H. Cai^{38,k,l}, X. Cai^{1,58}, A. Calcaterra^{28A}, G. F. Cao^{1,64}, N. Cao^{1,64}, S. A. Cetin^{62A}, X. Y. Chai^{46,h}, J. F. Chang^{1,58}, G. R. Che⁴³, Y. Z. Che^{1,58,64}, G. Chelkov^{36,b}, C. Chen⁴³, C. H. Chen⁹, Chao Chen⁵⁵, G. Chen¹, H. S. Chen^{1,64}, H. Y. Chen²⁰, M. L. Chen^{1,58,64}, S. J. Chen³⁴, Z. J. Chen^{25,i}, Z. K. Chen⁵⁹, S. K. Choi¹⁰, X. Chu^{12,g}, G. Cibinetto^{29A}, X. T. Chen^{1,64}, Y. B. Chen^{1,58}, Y. Q. Chen³⁴, Z. J. Chen^{25,i}, Z. K. Chen⁵⁹, S. K. Choi¹⁰, X. Chu^{12,g}, G. Cibinetto^{29A}, F. Cossio^{75C}, J. J. Cui⁵⁰, H. L. Dai^{1,58}, J. P. Dai⁷⁹, A. Dbeysi¹⁸, R. E. de Boer³, D. Dedovich³⁶, C. Q. Deng⁷³, Z. Y. Deng¹, A. Denig³⁵, I. Denysenko³⁶, M. Destefanis^{75A,75C}, F. De Mori^{75A,75C}, B. Ding^{67,1}, X. X. Ding^{46,h}, Y. Ding³⁴, Y. Ding⁴⁰, Y. X. Ding³⁰, J. Dong^{1,58}, L. Y. Dong^{1,64}, M. Y. Dong^{1,58,64}, X. Dong⁷⁷, M. C. Du¹, S. X. Du⁸¹, Y. Y. Duan⁵⁵, Z. H. Duan⁴², P. Egorov^{36,b}, G. F. Fan⁴², J. J. Fan¹⁹, Y. H. Fan⁴⁵, J. Fang⁵⁹, J. Fang^{1,58}, S. S. Fang^{1,64}, W. X. Fang¹, Y. Q. Fang^{1,58}, R. Farinelli^{29A}, L. Fava^{75B,75C}, F. Feldbauer³, G. Felici^{28A}, C. Q. Feng^{72,58}, J. H. Feng⁵⁹, Y. T. Feng^{72,58}, M. Fritsch³, C. D. Fu¹, J. L. Fu⁶⁴, Y. W. Fu^{1,64}, H. Gao⁶⁴, X. B. Gao⁴¹, Y. N. Gao^{46,h}, Y. N. Gao¹⁹, Y. Y. Gao³⁰, Yang Gao^{72,58}, S. Garbolino^{75C}, I. Garzia^{29A,29B}, P. T. Ge¹⁹, Z. W. Ge⁴², C. Geng⁵⁹, E. M. Gersabeck⁶⁸, A. Gilman⁷⁰, K. Goetzen¹³, J. D. Gong³⁴, L. Gong⁴⁰, W. X. Gong^{1,58}, W. Gradl³⁵, S. Gramigna^{29A,29B}, M. Greco^{75A,75C}, M. H. Gu^{1,58}, Y. T. Gu¹⁵, C. Y. Guan^{1,64}, A. Q. Guo³¹, L. B. Guo⁴¹, M. J. Guo⁵⁰, R. P. Guo⁴⁹, Y. P. Guo^{12,g}, A. Guskov^{36,b}, J. Gutierrez²⁷, K. L. Han⁶⁴, T. T. Han¹, F. Hanisch³, K. D. Hao^{72,58}, X. Q. Hao¹⁹, F. A. Harris⁶⁶, K. K. He⁵⁵, K. L. He^{1,64}, F. H. Heinsius³, C. H. Heinz³⁵, Y. K. Heng^{1,58,64}, C. Herold⁶⁰, T. Holtmann³, P. C. Hong³⁴, G. Y. Hou^{1,64}, X. T. Hou^{1,64}, Y. R. Hou⁶⁴, Z. L. Hou¹, B. Y. Hu⁵⁹, H. M. Hu^{1,64}, J. F. Hu^{56,j}, Q. P. Hu^{72,58}, S. L. Hu^{12,g}, T. Hu^{1,58,64}, Y. Hu¹, Z. M. Hu⁵⁹, G. S. Huang^{72,58}, K. X. Huang⁵⁹, L. Q. Huang^{31,64}, P. Huang⁴², X. T. Huang⁵⁰, Y. P. Huang¹, Y. S. Huang⁵⁹, T. Hussain⁷⁴, N. Hüsken³⁵, N. in der Wiesche⁶⁹, J. Jackson²⁷, S. Janchiv³², Q. Ji¹, Q. P. Ji¹⁹, W. Ji^{1,64}, X. B. Ji^{1,64}, X. L. Ji^{1,58}, Y. Y. Ji⁵⁰, Z. K. Jia^{72,58}, D. Jiang^{1,64}, H. B. Jiang⁷⁷, P. C. Jiang^{46,h}, S. J. Jiang⁹, T. J. Jiang¹⁶, X. S. Jiang^{1,58,64}, Y. Jiang⁶⁴, J. B. Jiao⁵⁰, J. K. Jiao³⁴, Z. Jiao²³, S. Jin⁴², Y. Jin⁶⁷, M. Q. Jing^{1,64}, X. M. Jing⁶⁴, T. Johansson⁷⁶, S. Kabana³³, N. Kalantar-Nayestanaki⁶⁵, X. L. Kang⁹, X. S. Kang⁴⁰, M. Kavatsyuk⁶⁵, B. C. Ke⁸¹, V. Khachatryan²⁷, A. Khoukaz⁶⁹, R. Kiuchi¹, O. B. Kolcu^{62A}, B. Kopf³, M. Kuessner³, X. Kui^{1,64}, N. Kumar²⁶, A. Kupsc^{44,76}, W. Kühn³⁷, Q. Lan⁷³, W. N. Lan¹⁹, T. T. Lei^{72,58}, M. Lellmann³⁵, T. Lenz³⁵, C. Li⁴³, C. Li⁴⁷, C. H. Li³⁹, C. K. Li²⁰, Cheng Li^{72,58}, D. M. Li⁸¹, F. Li^{1,58}, G. Li¹, H. B. Li^{1,64}, H. J. Li¹⁹, H. N. Li^{56,j}, Hui Li⁴³, J. R. Li⁶¹, J. S. Li⁵⁹, K. Li¹, K. L. Li^{38,k,l}, K. L. Li¹⁹, L. J. Li^{1,64}, Lei Li⁴⁸, M. H. Li⁴³, M. R. Li^{1,64}, P. L. Li⁶⁴, P. R. Li^{38,k,l}, Q. M. Li^{1,64}, Q. X. Li⁵⁰, R. Li^{17,31}, T. Li⁵⁰, T. Y. Li⁴³, W. D. Li^{1,64}, W. G. Li^{1,a}, X. Li^{1,64}, X. H. Li^{72,58}, X. L. Li⁵⁰, X. Y. Li^{1,8}, X. Z. Li⁵⁹, Y. Li¹⁹, Y. G. Li^{46,h}, Y. P. Li³⁴, Z. J. Li⁵⁹, Z. Y. Li⁷⁹, C. Liang⁴², H. Liang^{72,58}, Y. F. Liang⁵⁴, Y. T. Liang^{31,64}, G. R. Liao¹⁴, L. B. Liao⁵⁹, M. H. Liao⁵⁹, Y. P. Liao^{1,64}, J. Libby²⁶, A. Limphirat⁶⁰, C. C. Lin⁵⁵, C. X. Lin⁶⁴, D. X. Lin^{31,64}, L. Q. Lin³⁹, T. Lin¹, B. J. Liu¹, B. X. Liu⁷⁷, C. Liu³⁴, C. X. Liu¹, F. Liu¹, F. H. Liu⁵³, Feng Liu⁶, G. M. Liu^{56,j}, H. Liu^{38,k,l}, H. B. Liu¹⁵, H. H. Liu¹, H. M. Liu^{1,64}, Huihui Liu²¹, J. B. Liu^{72,58}, J. J. Liu²⁰, K. Liu^{38,k,l}, K. Liu⁷³, K. Y. Liu⁴⁰, Ke Liu²², L. Liu^{72,58}, L. C. Liu⁴³, Lu Liu⁴³, P. L. Liu¹, Q. Liu⁶⁴, S. B. Liu^{72,58}, T. Liu^{12,g}, W. K. Liu⁴³, W. M. Liu^{72,58}, W. T. Liu³⁹, X. Liu^{38,k,l}, X. Liu³⁹, X. Y. Liu⁷⁷, Y. Liu^{38,k,l}, Y. Liu⁸¹, Y. Liu⁸¹, Y. B. Liu⁴³, Z. A. Liu^{1,58,64}, Z. D. Liu⁹, Z. Q. Liu⁵⁰, X. C. Lou^{1,58,64}, F. X. Lu⁵⁹, H. J. Lu²³, J. G. Lu^{1,58}, Y. Lu⁷, Y. H. Lu^{1,64}, Y. P. Lu^{1,58}, Z. H. Lu^{1,64}, C. L. Luo⁴¹, J. R. Luo⁵⁹, J. S. Luo^{1,64}, M. X. Luo⁸⁰, T. Luo^{12,g}, X. L. Luo^{1,58}, Z. Y. Lv²², X. R. Lyu^{64,p}, Y. F. Lyu⁴³, Y. H. Lyu⁸¹, F. C. Ma⁴⁰, H. Ma⁷⁹, H. L. Ma¹, J. L. Ma^{1,64}, L. L. Ma⁵⁰, L. R. Ma⁶⁷, Q. M. Ma¹, R. Q. Ma^{1,64}, R. Y. Ma¹⁹, T. Ma^{72,58}, X. T. Ma^{1,64}, X. Y. Ma^{1,58}, Y. M. Ma³¹, F. E. Maas¹⁸, I. MacKay⁷⁰, M. Maggiora^{75A,75C}, S. Malde⁷⁰, Y. J. Mao^{46,h}, Z. P. Mao¹, S. Marcello^{75A,75C}, F. M. Melendi^{29A,29B}, Y. H. Meng⁶⁴, Z. X. Meng⁶⁷, J. G. Messchendorp^{13,65}, G. Mezzadri^{29A}, H. Miao^{1,64}, T. J. Min⁴², R. E. Mitchell²⁷, X. H. Mo^{1,58,64}, B. Moses²⁷, N. Yu. Muchnoi^{4,c}, J. Muskalla³⁵, Y. Nefedov³⁶, F. Nerling^{18,e}, L. S. Nie²⁰, I. B. Nikolaev^{4,c}, Z. Ning^{1,58}, S. Nisar^{11,m}, Q. L. Niu^{38,k,l}, W. D. Niu^{12,g}, S. L. Olsen^{10,64}, Q. Ouyang^{1,58,64}, S. Pacetti^{28B,28C}, X. Pan⁵⁵, Y. Pan⁵⁷, A. Pathak¹⁰, Y. P. Pei^{72,58}, M. Pelizaeus³, H. P. Peng^{72,58}, Y. Y. Peng^{38,k,l}, K. Peters^{13,e}, J. L. Ping⁴¹, R. G. Ping^{1,64}, S. Plura³⁵, V. Prasad³³, F. Z. Qi¹, H. R. Qi⁶¹, M. Qi⁴², S. Qian^{1,58}, W. B. Qian⁶⁴, C. F. Qiao⁶⁴, J. H. Qiao¹⁹, J. J. Qin⁷³, J. L. Qin⁵⁵, L. Q. Qin¹⁴, L. Y. Qin^{72,58}, P. B. Qin⁷³, X. P. Qin^{12,g}, X. S. Qin⁵⁰, Z. H. Qin^{1,58}, J. F. Qiu¹, Z. H. Qu⁷³, C. F. Redmer³⁵, A. Rivetti^{75C}, M. Rolo^{75C}, G. Rong^{1,64}, S. S. Rong^{1,64}, F. Rosini^{28B,28C}, Ch. Rosner¹⁸, M. Q. Ruan^{1,58}, S. N. Ruan⁴³, N. Salone⁴⁴, A. Sarantsev^{36,d}, Y. Schelhaas³⁵, K. Schoenning⁷⁶, M. Scodeggio^{29A}, K. Y. Shan^{12,g}, W. Shan²⁴, X. Y. Shan^{72,58}, Z. J. Shang^{38,k,l}, J. F. Shanguan¹⁶, L. G. Shao^{1,64}, M. Shao^{72,58}, C. P. Shen^{12,g}, H. F. Shen^{1,8}, W. H. Shen⁶⁴, X. Y. Shen^{1,64}, B. A. Shi⁶⁴, H. Shi^{72,58}, J. L. Shi^{12,g}, J. Y. Shi¹, S. Y. Shi⁷³, X. Shi^{1,58}, H. L. Song^{72,58}, J. J. Song¹⁹, T. Z. Song⁵⁹, W. M. Song^{34,1}, Y. X. Song^{46,h,n}, S. Sosio^{75A,75C}, S. Spataro^{75A,75C}, F. Stieler³⁵, S. S. Su⁴⁰, Y. J. Su⁶⁴, G. B. Sun⁷⁷, G. X. Sun¹, H. Sun⁶⁴, H. K. Sun¹, J. F. Sun¹⁹, K. Sun⁶¹, L. Sun⁷⁷, S. S. Sun^{1,64}, T. Sun^{51,f}, Y. C. Sun⁷⁷, Y. H. Sun³⁰, Y. J. Sun^{72,58}, Y. Z. Sun¹, Z. Q. Sun^{1,64}, Z. T. Sun⁵⁰, C. J. Tang⁵⁴, G. Y. Tang¹, J. Tang⁵⁹, L. F. Tang³⁹, M. Tang^{72,58}, Y. A. Tang⁷⁷, L. Y. Tao⁷³, M. Tat⁷⁰, J. X. Teng^{72,58}, J. Y. Tian^{72,58}, W. H. Tian⁵⁹, Y. Tian³¹, Z. F. Tian⁷⁷, I. Uman^{62B}, B. Wang^{1,58}, L. L. Wang¹, L. W. Wang³⁴, C. Wang¹⁹, Cong Wang²², D. Y. Wang^{46,h}, H. J. Wang^{38,k,l}, J. J. Wang⁷⁷, K. Wang^{1,58}, L. W. Wang¹, L. W. Wang³⁴, M. Wang⁵⁰, M. Wang^{72,58}, N. Y. Wang⁶⁴, S. Wang^{12,g}, T. Wang^{12,g}, T. J. Wang⁴³, W. Wang⁷³, W. Wang⁵⁹, W. P. Wang^{35,58,72,o}, X. Wang^{46,h}, X. F. Wang^{38,k,l}, X. J. Wang³⁹, X. L. Wang^{12,g}, X. N. Wang¹, Y. Wang⁶¹, Y. D. Wang⁴⁵, Y. F. Wang^{1,58,64}, Y. H. Wang^{38,k,l}, Y. L. Wang¹⁹, Y. N. Wang⁷⁷, Y. Q. Wang¹, Yaqian Wang¹⁷, Yi Wang⁶¹, Yuan Wang^{17,31}, Z. Wang^{1,58}, Z. L. Wang⁷³, Z. L. Wang², Z. Q. Wang^{12,g}, Z. Y. Wang^{1,64}, D. H. Wei¹⁴, H. R. Wei⁴³, F. Weidner⁶⁹, S. P. Wen¹, Y. R. Wen³⁹, U. Wiedner³, G. Wilkinson⁷⁰, M. Wolke⁷⁶, C. Wu³⁹, J. F. Wu^{1,8}, L. H. Wu¹, L. J. Wu^{1,64}, Lianjie Wu¹⁹, S. G. Wu^{1,64}, S. M. Wu⁶⁴, X. Wu^{12,g}, X. H. Wu³⁴, Y. J. Wu³¹, Z. Wu^{1,58}, L. Xia^{72,58},

X. M. Xian³⁹, B. H. Xiang^{1,64}, T. Xiang^{46,h}, D. Xiao^{38,k,l}, G. Y. Xiao⁴², H. Xiao⁷³, Y. L. Xiao^{12,g}, Z. J. Xiao⁴¹, C. Xie⁴², K. J. Xie^{1,64}, X. H. Xie^{46,h}, Y. Xie⁵⁰, Y. G. Xie^{1,58}, Y. H. Xie⁶, Z. P. Xie^{72,58}, T. Y. Xing^{1,64}, C. F. Xu^{1,64}, C. J. Xu⁵⁹, G. F. Xu¹, H. Y. Xu², H. Y. Xu^{67,2}, M. Xu^{72,58}, Q. J. Xu¹⁶, Q. N. Xu³⁰, W. L. Xu⁶⁷, X. P. Xu⁵⁵, Y. Xu⁴⁰, Y. Xu^{12,g}, Y. C. Xu⁷⁸, Z. S. Xu⁶⁴, H. Y. Yan³⁹, L. Yan^{12,g}, W. B. Yan^{72,58}, W. C. Yan⁸¹, W. P. Yan¹⁹, X. Q. Yan^{1,64}, H. J. Yang^{51,f}, H. L. Yang³⁴, H. X. Yang¹, J. H. Yang⁴², R. J. Yang¹⁹, T. Yang¹, Y. Yang^{12,g}, Y. F. Yang⁴³, Y. H. Yang⁴², Y. Q. Yang⁹, Y. X. Yang^{1,64}, Y. Z. Yang¹⁹, M. Ye^{1,58}, M. H. Ye⁸, Junhao Yin⁴³, Z. Y. You⁵⁹, B. X. Yu^{1,58,64}, C. X. Yu⁴³, G. Yu¹³, J. S. Yu^{25,i}, M. C. Yu⁴⁰, T. Yu⁷³, X. D. Yu^{46,h}, Y. C. Yu⁸¹, C. Z. Yuan^{1,64}, H. Yuan^{1,64}, J. Yuan⁴⁵, J. Yuan³⁴, L. Yuan², S. C. Yuan^{1,64}, Y. Yuan^{1,64}, Z. Y. Yuan⁵⁹, C. X. Yue³⁹, Ying Yue¹⁹, A. A. Zafar⁷⁴, S. H. Zeng^{63A,63B,63C,63D}, X. Zeng^{12,g}, Y. Zeng^{25,i}, Y. J. Zeng^{1,64}, Y. J. Zeng⁵⁹, X. Y. Zhai³⁴, Y. H. Zhan⁵⁹, A. Q. Zhang^{1,64}, B. L. Zhang^{1,64}, B. X. Zhang¹, D. H. Zhang⁴³, G. Y. Zhang¹⁹, G. Y. Zhang^{1,64}, H. Zhang^{72,58}, H. Zhang⁸¹, H. C. Zhang^{1,58,64}, H. H. Zhang⁵⁹, H. Q. Zhang^{1,58,64}, H. R. Zhang^{72,58}, H. Y. Zhang^{1,58}, J. Zhang⁵⁹, J. Zhang⁸¹, J. J. Zhang⁵², J. L. Zhang²⁰, J. Q. Zhang⁴¹, J. S. Zhang^{12,g}, J. W. Zhang^{1,58,64}, J. X. Zhang^{38,k,l}, J. Y. Zhang¹, J. Z. Zhang^{1,64}, Jianyu Zhang⁶⁴, L. M. Zhang⁶¹, Lei Zhang⁴², N. Zhang⁸¹, P. Zhang^{1,64}, Q. Zhang¹⁹, Q. Y. Zhang³⁴, R. Y. Zhang^{38,k,l}, S. H. Zhang^{1,64}, Shulei Zhang^{25,i}, X. M. Zhang¹, X. Y. Zhang⁴⁰, X. Y. Zhang⁵⁰, Y. Zhang⁷³, Y. Zhang¹, Y. T. Zhang⁸¹, Y. H. Zhang^{1,58}, Y. M. Zhang³⁹, Z. D. Zhang¹, Z. H. Zhang¹, Z. L. Zhang³⁴, Z. L. Zhang⁵⁵, Z. X. Zhang¹⁹, Z. Y. Zhang⁴³, Z. Y. Zhang⁷⁷, Z. Z. Zhang⁴⁵, Zh. Zh. Zhang¹⁹, G. Zhao¹, J. Y. Zhao^{1,64}, J. Z. Zhao^{1,58}, L. Zhao¹, Lei Zhao^{72,58}, M. G. Zhao⁴³, N. Zhao⁷⁹, R. P. Zhao⁶⁴, S. J. Zhao⁸¹, Y. B. Zhao^{1,58}, Y. L. Zhao⁵⁵, Y. X. Zhao^{31,64}, Z. G. Zhao^{72,58}, A. Zhemchugov^{36,b}, B. Zheng⁷³, B. M. Zheng³⁴, J. P. Zheng^{1,58}, W. J. Zheng^{1,64}, X. R. Zheng¹⁹, Y. H. Zheng^{64,p}, B. Zhong⁴¹, X. Zhong⁵⁹, H. Zhou^{35,50,o}, J. Q. Zhou³⁴, J. Y. Zhou³⁴, S. Zhou⁶, X. Zhou⁷⁷, X. K. Zhou⁶, X. R. Zhou^{72,58}, X. Y. Zhou³⁹, Y. Z. Zhou^{12,g}, Z. C. Zhou²⁰, A. N. Zhu⁶⁴, J. Zhu⁴³, K. Zhu¹, K. J. Zhu^{1,58,64}, K. S. Zhu^{12,g}, L. Zhu³⁴, L. X. Zhu⁶⁴, S. H. Zhu⁷¹, T. J. Zhu^{12,g}, W. D. Zhu^{12,g}, W. D. Zhu⁴¹, W. J. Zhu¹, W. Z. Zhu¹⁹, Y. C. Zhu^{72,58}, Z. A. Zhu^{1,64}, X. Y. Zhuang⁴³, J. H. Zou¹, J. Zu^{72,58}

(BESIII Collaboration)

¹ Institute of High Energy Physics, Beijing 100049, People's Republic of China

² Beihang University, Beijing 100191, People's Republic of China

³ Bochum Ruhr-University, D-44780 Bochum, Germany

⁴ Budker Institute of Nuclear Physics SB RAS (BINP), Novosibirsk 630090, Russia

⁵ Carnegie Mellon University, Pittsburgh, Pennsylvania 15213, USA

⁶ Central China Normal University, Wuhan 430079, People's Republic of China

⁷ Central South University, Changsha 410083, People's Republic of China

⁸ China Center of Advanced Science and Technology, Beijing 100190, People's Republic of China

⁹ China University of Geosciences, Wuhan 430074, People's Republic of China

¹⁰ Chung-Ang University, Seoul, 06974, Republic of Korea

¹¹ COMSATS University Islamabad, Lahore Campus, Defence Road, Off Raiwind Road, 54000 Lahore, Pakistan

¹² Fudan University, Shanghai 200433, People's Republic of China

¹³ GSI Helmholtzcentre for Heavy Ion Research GmbH, D-64291 Darmstadt, Germany

¹⁴ Guangxi Normal University, Guilin 541004, People's Republic of China

¹⁵ Guangxi University, Nanning 530004, People's Republic of China

¹⁶ Hangzhou Normal University, Hangzhou 310036, People's Republic of China

¹⁷ Hebei University, Baoding 071002, People's Republic of China

¹⁸ Helmholtz Institute Mainz, Staudinger Weg 18, D-55099 Mainz, Germany

¹⁹ Henan Normal University, Xinxiang 453007, People's Republic of China

²⁰ Henan University, Kaifeng 475004, People's Republic of China

²¹ Henan University of Science and Technology, Luoyang 471003, People's Republic of China

²² Henan University of Technology, Zhengzhou 450001, People's Republic of China

²³ Huangshan College, Huangshan 245000, People's Republic of China

²⁴ Hunan Normal University, Changsha 410081, People's Republic of China

²⁵ Hunan University, Changsha 410082, People's Republic of China

²⁶ Indian Institute of Technology Madras, Chennai 600036, India

²⁷ Indiana University, Bloomington, Indiana 47405, USA

²⁸ INFN Laboratori Nazionali di Frascati, (A)INFN Laboratori Nazionali di Frascati, I-00044, Frascati, Italy; (B)INFN

Sezione di Perugia, I-06100, Perugia, Italy; (C)University of Perugia, I-06100, Perugia, Italy

²⁹ INFN Sezione di Ferrara, (A)INFN Sezione di Ferrara, I-44122, Ferrara, Italy; (B)University of Ferrara, I-44122, Ferrara, Italy

³⁰ Inner Mongolia University, Hohhot 010021, People's Republic of China

³¹ Institute of Modern Physics, Lanzhou 730000, People's Republic of China

³² Institute of Physics and Technology, Peace Avenue 54B, Ulaanbaatar 13330, Mongolia

³³ Instituto de Alta Investigación, Universidad de Tarapacá, Casilla 7D, Arica 1000000, Chile

³⁴ Jilin University, Changchun 130012, People's Republic of China

³⁵ Johannes Gutenberg University of Mainz, Johann-Joachim-Becher-Weg 45, D-55099 Mainz, Germany

³⁶ Joint Institute for Nuclear Research, 141980 Dubna, Moscow region, Russia

³⁷ Justus-Liebig-Universität Giessen, II. Physikalisches Institut, Heinrich-Buff-Ring 16, D-35392 Giessen, Germany

³⁸ Lanzhou University, Lanzhou 730000, People's Republic of China

- ³⁹ Liaoning Normal University, Dalian 116029, People's Republic of China
- ⁴⁰ Liaoning University, Shenyang 110036, People's Republic of China
- ⁴¹ Nanjing Normal University, Nanjing 210023, People's Republic of China
- ⁴² Nanjing University, Nanjing 210093, People's Republic of China
- ⁴³ Nankai University, Tianjin 300071, People's Republic of China
- ⁴⁴ National Centre for Nuclear Research, Warsaw 02-093, Poland
- ⁴⁵ North China Electric Power University, Beijing 102206, People's Republic of China
- ⁴⁶ Peking University, Beijing 100871, People's Republic of China
- ⁴⁷ Qufu Normal University, Qufu 273165, People's Republic of China
- ⁴⁸ Renmin University of China, Beijing 100872, People's Republic of China
- ⁴⁹ Shandong Normal University, Jinan 250014, People's Republic of China
- ⁵⁰ Shandong University, Jinan 250100, People's Republic of China
- ⁵¹ Shanghai Jiao Tong University, Shanghai 200240, People's Republic of China
- ⁵² Shanxi Normal University, Linfen 041004, People's Republic of China
- ⁵³ Shanxi University, Taiyuan 030006, People's Republic of China
- ⁵⁴ Sichuan University, Chengdu 610064, People's Republic of China
- ⁵⁵ Soochow University, Suzhou 215006, People's Republic of China
- ⁵⁶ South China Normal University, Guangzhou 510006, People's Republic of China
- ⁵⁷ Southeast University, Nanjing 211100, People's Republic of China
- ⁵⁸ State Key Laboratory of Particle Detection and Electronics, Beijing 100049, Hefei 230026, People's Republic of China
- ⁵⁹ Sun Yat-Sen University, Guangzhou 510275, People's Republic of China
- ⁶⁰ Suranaree University of Technology, University Avenue 111, Nakhon Ratchasima 30000, Thailand
- ⁶¹ Tsinghua University, Beijing 100084, People's Republic of China
- ⁶² Turkish Accelerator Center Particle Factory Group, (A)Istinye University, 34010, Istanbul, Turkey; (B)Near East University, Nicosia, North Cyprus, 99138, Mersin 10, Turkey
- ⁶³ University of Bristol, H H Wills Physics Laboratory, Tyndall Avenue, Bristol, BS8 1TL, UK
- ⁶⁴ University of Chinese Academy of Sciences, Beijing 100049, People's Republic of China
- ⁶⁵ University of Groningen, NL-9747 AA Groningen, The Netherlands
- ⁶⁶ University of Hawaii, Honolulu, Hawaii 96822, USA
- ⁶⁷ University of Jinan, Jinan 250022, People's Republic of China
- ⁶⁸ University of Manchester, Oxford Road, Manchester, M13 9PL, United Kingdom
- ⁶⁹ University of Muenster, Wilhelm-Klemm-Strasse 9, 48149 Muenster, Germany
- ⁷⁰ University of Oxford, Keble Road, Oxford OX13RH, United Kingdom
- ⁷¹ University of Science and Technology Liaoning, Anshan 114051, People's Republic of China
- ⁷² University of Science and Technology of China, Hefei 230026, People's Republic of China
- ⁷³ University of South China, Hengyang 421001, People's Republic of China
- ⁷⁴ University of the Punjab, Lahore-54590, Pakistan
- ⁷⁵ University of Turin and INFN, (A)University of Turin, I-10125, Turin, Italy; (B)University of Eastern Piedmont, I-15121, Alessandria, Italy; (C)INFN, I-10125, Turin, Italy
- ⁷⁶ Uppsala University, Box 516, SE-75120 Uppsala, Sweden
- ⁷⁷ Wuhan University, Wuhan 430072, People's Republic of China
- ⁷⁸ Yantai University, Yantai 264005, People's Republic of China
- ⁷⁹ Yunnan University, Kunming 650500, People's Republic of China
- ⁸⁰ Zhejiang University, Hangzhou 310027, People's Republic of China
- ⁸¹ Zhengzhou University, Zhengzhou 450001, People's Republic of China
- ^a Deceased
- ^b Also at the Moscow Institute of Physics and Technology, Moscow 141700, Russia
- ^c Also at the Novosibirsk State University, Novosibirsk, 630090, Russia
- ^d Also at the NRC "Kurchatov Institute", PNPI, 188300, Gatchina, Russia
- ^e Also at Goethe University Frankfurt, 60323 Frankfurt am Main, Germany
- ^f Also at Key Laboratory for Particle Physics, Astrophysics and Cosmology, Ministry of Education; Shanghai Key Laboratory for Particle Physics and Cosmology; Institute of Nuclear and Particle Physics, Shanghai 200240, People's Republic of China
- ^g Also at Key Laboratory of Nuclear Physics and Ion-beam Application (MOE) and Institute of Modern Physics, Fudan University, Shanghai 200443, People's Republic of China
- ^h Also at State Key Laboratory of Nuclear Physics and Technology, Peking University, Beijing 100871, People's Republic of China
- ⁱ Also at School of Physics and Electronics, Hunan University, Changsha 410082, China
- ^j Also at Guangdong Provincial Key Laboratory of Nuclear Science, Institute of Quantum Matter, South China Normal University, Guangzhou 510006, China
- ^k Also at MOE Frontiers Science Center for Rare Isotopes, Lanzhou University, Lanzhou 730000, People's Republic of China
- ^l Also at Lanzhou Center for Theoretical Physics, Lanzhou University, Lanzhou 730000, People's Republic of China
- ^m Also at the Department of Mathematical Sciences, IBA, Karachi 75270, Pakistan
- ⁿ Also at Ecole Polytechnique Federale de Lausanne (EPFL), CH-1015 Lausanne, Switzerland

^o Also at Helmholtz Institute Mainz, Staudinger Weg 18, D-55099 Mainz, Germany

^p Also at Hangzhou Institute for Advanced Study, University of Chinese Academy of Sciences, Hangzhou 310024, China

The non-leptonic two-body weak decays $\Sigma^+ \rightarrow p\pi^0$ and $\bar{\Sigma}^- \rightarrow \bar{p}\pi^0$ are investigated, utilizing $(1.0087 \pm 0.0044) \times 10^{10}$ J/ψ events and $(2.7124 \pm 0.0143) \times 10^9$ $\psi(3686)$ events collected by BESIII experiment. The precision of the weak-decay parameters for the decays $\Sigma^+ \rightarrow p\pi^0$ (α_0) and $\bar{\Sigma}^- \rightarrow \bar{p}\pi^0$ ($\bar{\alpha}_0$) is improved by a factor of three compared to the previous world average. Furthermore, the quantum-entangled $\Sigma^+\bar{\Sigma}^-$ system enables the most precise test of CP symmetry for the decay $\Sigma^+ \rightarrow p\pi^0$, through the asymmetry observable $A_{CP} = (\alpha_0 + \bar{\alpha}_0)/(\alpha_0 - \bar{\alpha}_0)$ that is measured to be $-0.0118 \pm 0.0083_{\text{stat}} \pm 0.0028_{\text{sys}}$. Assuming CP conservation, the average decay parameter is determined to be $\langle \alpha_0 \rangle = (\alpha_0 - \bar{\alpha}_0)/2 = -0.9869 \pm 0.0011_{\text{stat}} \pm 0.0016_{\text{sys}}$, which is the most precise measurement of the asymmetry decay parameters in baryon sectors. The angular dependence of the ratio of the polarization of the Σ^+ in both J/ψ and $\psi(3686)$ decays is studied for the first time.

Violation of charge conjugation and parity (CP) symmetry is one of the three fundamental conditions to explain the abundance of matter with respect to antimatter in the universe [1]. CP violation has been observed in decays of K , B and D mesons and is described theoretically in the Standard Model (SM) of particle physics through the Kobayashi-Maskawa mechanism [2–9]. In addition, there has also been recent evidence suggesting the existence of CP violation in Λ_b^0 decay [10]. However, the observed violations of CP symmetry in these processes are not sufficient to explain the matter-antimatter asymmetry of the universe [11], implying the existence of sources of sizable CP violation beyond the SM (BSM) [12–16]. Hyperon weak decays have recently been shown to be a promising hunting-ground for CP -violating processes. In these decays parity violation is described by non-zero values of the decay parameters α_h and $\bar{\alpha}_h$ for hyperons and anti-hyperons, respectively [17]. CP symmetry can be tested experimentally by defining the CP -odd asymmetry [18–21]

$$A_{CP} = (\alpha_h + \bar{\alpha}_h)/(\alpha_h - \bar{\alpha}_h), \quad (1)$$

where a value significantly deviating from zero would indicate CP violation. Predictions for the $A_{CP}(\Sigma^+ \rightarrow p\pi^0)$ asymmetry in the SM vary between -3.2×10^{-7} [22] and 3.6×10^{-6} [23]. Several BSM theories predict an order of magnitude larger values, for example -3.2×10^{-5} with the Weinberg-Higgs model and -2.9×10^{-5} with the left-right-symmetric model [22]. In 2020, the BESIII collaboration measured this asymmetry for the first time, reporting $A_{CP}(\Sigma^+ \rightarrow p\pi^0) = 0.004 \pm 0.037 \pm 0.010$ [21], which is consistent with CP conservation. The measurement was based on 1.311×10^9 J/ψ and 4.481×10^8 $\psi(3686)$ events [24, 25]. However, to test the aforementioned theoretical predictions and to search for the potential BSM physics, more precise measurements are needed.

The decay asymmetries that these tests rely upon are experimentally accessible through the angular distribution of the decaying hadron. For a spin-1/2 hyperon decaying into a spin-1/2 baryon and a pseudoscalar meson,

the angular distribution is described by

$$dN/d\Omega = \frac{1}{4\pi}(1 + \alpha_h \cdot |\vec{\mathbf{P}}_h| \cdot \cos\theta_P), \quad (2)$$

where $\vec{\mathbf{P}}_h$ is the hyperon polarization, and θ_P is the angle between the polarization direction and the direction of the final state baryon in the hyperon rest frame. The decay parameter α_h is interesting in its own right. Since it is related to the hyperon matrix element, it gives insight to the SU(3)-flavour structure and the symmetry-breaking patterns of the quark distributions [26]. The non-perturbative nature of the strong-decay amplitudes makes this parameter challenging to calculate. Effective field theories [27] and quark or diquark models [28] have been applied with a varying degree of success. Recent progress in Lattice QCD [26], where calculations of hyperon decay amplitudes are foreseen, opens up the possibility to understand hyperon decays in a more coherent way.

Predictions of the spin properties of heavy multi-strange, charm and beauty baryons rely on precise knowledge of the decay parameters of the light hyperons that they decay into. This is not only true for CP tests of heavy hyperons and baryons [29–32], but also for nuclear and hadron physics, where they are crucial components for understanding the spin structure of hyperons [33–35], the vortex structure [36], and the magnetic-field distribution in quark-gluon plasma (QGP) [37]. Recent experiments, such as the STAR experiment on Λ hyperon polarization in Au+Au collisions [38] and the Belle collaboration’s measurement of the transverse polarization of hyperons from quark-antiquark fragmentation [39], have revealed key insights. However, none of these studies employed the Σ^+ baryon as a probe. In summary, there are many motivations for performing precise measurements of the decay parameters of $\Sigma^+ \rightarrow p\pi^0$ and $\bar{\Sigma}^- \rightarrow \bar{p}\pi^0$.

In the BESIII experiment, the polarized hyperon and anti-hyperon pairs are produced through e^+e^- annihilation, providing a unique environment for studying the production and its decay properties of this system. The decay parameters and A_{CP} can be measured precisely

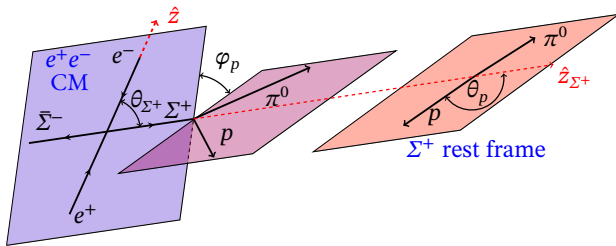


Figure 1. The helicity frame definition for the decay processes $\Psi \rightarrow \Sigma^+\bar{\Sigma}^-$, $\Sigma^+ \rightarrow p\pi^0$, $\bar{\Sigma}^- \rightarrow \bar{p}\pi^0$ in the center-of-mass (CM) system of the e^+e^- collision. The helicity angles are defined with respect to the direction of the outgoing hyperon in the CM frame, where \hat{z}_{Σ^+} is defined along the Σ^+ momentum direction in the CM of the e^+e^- collision.

due to the Σ^+ and $\bar{\Sigma}^-$ being in a quantum-entangled state with correlated spin. The full process $e^+e^- \rightarrow \Psi \rightarrow \Sigma^+\bar{\Sigma}^- \rightarrow p\pi^0\bar{p}\pi^0$ can be described by the helicity angles of the final-state particles, an angular-distribution parameter α_Ψ , a relative phase $\Delta\Phi$, and two decay parameters [40–43]. As seen from the basis vector definitions in Fig. 1, θ_{Σ^+} is the angle between the Σ^+ momentum and the electron-beam direction, and θ_p and ϕ_p are the polar and azimuthal angles of the p momentum direction in the Σ^+ rest frame. The joint angular distribution $\mathcal{W}(\boldsymbol{\xi})$ [40, 43, 44] of the $e^+e^- \rightarrow \Psi \rightarrow \Sigma^+\bar{\Sigma}^-$, $\Sigma^+ \rightarrow p\pi^0$, and $\bar{\Sigma}^- \rightarrow \bar{p}\pi^0$ processes is given by

$$\begin{aligned} \mathcal{W}(\boldsymbol{\xi}) = & \mathcal{T}_0(\boldsymbol{\xi}) + \alpha_\Psi \mathcal{T}_5(\boldsymbol{\xi}) \\ & + \alpha_0 \bar{\alpha}_0 \left(\mathcal{T}_1(\boldsymbol{\xi}) + \sqrt{1 - \alpha_\Psi^2} \cos(\Delta\Phi) \mathcal{T}_2(\boldsymbol{\xi}) + \alpha_\Psi \mathcal{T}_6(\boldsymbol{\xi}) \right) \\ & + \sqrt{1 - \alpha_\Psi^2} \sin(\Delta\Phi) (\alpha_0 \mathcal{T}_3(\boldsymbol{\xi}) + \bar{\alpha}_0 \mathcal{T}_4(\boldsymbol{\xi})), \end{aligned} \quad (3)$$

where Ψ signifies J/ψ or $\psi(3686)$, $\boldsymbol{\xi}$ denotes the polar angle and azimuthal angle of the particle in its final state, \mathcal{T}_k ($k = 0, 1, \dots, 6$) is a set of seven angular functions, and α_0 ($\bar{\alpha}_0$) is the decay parameter of $\Sigma^+ \rightarrow p\pi^0$ ($\bar{\Sigma}^- \rightarrow \bar{p}\pi^0$). The explicit dependence on the decay parameters α_0 and $\bar{\alpha}_0$ enables their simultaneous extraction. Equation 3 consists of three main contributions: one unpolarized part (involving \mathcal{T}_0 and \mathcal{T}_5) describing the scattering angular distribution, one part (with \mathcal{T}_1 , \mathcal{T}_2 and \mathcal{T}_6) describing the spin correlation between the Σ^+ and the $\bar{\Sigma}^-$, and finally the spin polarization of the Σ^+ and $\bar{\Sigma}^-$ (with \mathcal{T}_3 and \mathcal{T}_4 , respectively). The spin-correlated part and the spin-polarization part are governed by the psionic form-factor phase $\Delta\Phi$ and depends on the Σ^+ scattering angle via:

$$\vec{\mathbf{P}}_h(\cos \theta_{\Sigma^+}) = \frac{\sqrt{1 - \alpha_\Psi^2} \sin(\Delta\Phi) \cos \theta_{\Sigma^+} \sin \theta_{\Sigma^+}}{1 + \alpha_\Psi \cos^2 \theta_{\Sigma^+}}. \quad (4)$$

A non-zero phase $\Delta\Phi$ means that the Σ^+ and $\bar{\Sigma}^-$ hyperons are polarized even if the initial state is unpolarized.

The BESIII experiment has now accumulated $(1.0087 \pm 0.0044) \times 10^{10}$ J/ψ events [46] and $(2.7124 \pm 0.0143) \times 10^9$ $\psi(3686)$ events [45], which are 7.7 and 6.1

times larger, respectively, than the samples used in the previous measurement [21]. This opens unique and excellent opportunity for a new generation of high-precision CP tests, as already demonstrated in several recent papers [19, 20, 47]. Details about the design and performance of the BESIII detector at the BEPCII collider are given in Ref. [48].

The full reaction, including all subsequent decays, is $e^+e^- \rightarrow \Psi \rightarrow \Sigma^+\bar{\Sigma}^- \rightarrow p\bar{p}\pi^0\pi^0 \rightarrow p\bar{p}\gamma\gamma\gamma\gamma$. Selected event candidates are required to have two well-reconstructed charged tracks with net zero charge. Charged tracks detected in the multi-layer drift chamber (MDC) are required to be within a polar angle (θ) range of $|\cos\theta| < 0.93$, where θ is defined with respect to the z -axis, which is the symmetry axis of the MDC. For each charged track, the distance of closest approach to the interaction point (IP) must be less than 10 cm along the z -axis, and less than 2 cm in the transverse plane. Particle identification (PID) for charged tracks combines measurements of the specific ionization energy loss in the MDC (dE/dx) and the flight time in the time-of-flight to form likelihoods $\mathcal{L}(h)$ ($h = p, K, \pi$) for each hadron h hypothesis. Tracks are identified as protons or anti-protons when these hypotheses have the greatest likelihood ($\mathcal{L}(p) > \mathcal{L}(K)$ and $\mathcal{L}(p) > \mathcal{L}(\pi)$). The distance of closest approaches of the proton and anti-proton tracks to the IP is required to be larger than 0.34 cm, a distance optimized to suppress background events directly generated from the IP.

Photon candidates are identified using showers in the electromagnetic calorimeter (EMC). The deposited energy of each shower must be more than 25 MeV in the barrel region ($|\cos\theta| < 0.80$) and more than 50 MeV in the end-cap region ($0.86 < |\cos\theta| < 0.92$). To exclude showers originating from the charged tracks, the opening angle subtended by the EMC shower and the position of the closest charged track at the EMC must be greater than 10° as measured from the IP. To suppress electronic noise and showers unrelated to the signal event, the difference between the EMC time and the event start-time is required to be within $[0, 700]$ ns. To identify the π^0 candidates, the invariant mass $M_{\gamma\gamma}$ of the two photons has to satisfy $0.115 < M_{\gamma\gamma} < 0.150$ GeV/ c^2 . In addition, a one-constraint (1C) kinematic fit is performed to constrain $M_{\gamma\gamma}$ to the known π^0 mass [49]. The χ^2_{1C} of the fit is required to be smaller than 200. At least one π^0 candidate per event is selected. To further refine the selection, a two-constraint (2C) kinematic fit is performed to the decay $\Psi \rightarrow p\pi^0\bar{p}\pi^0$, utilizing four-momentum conservation in the decay and the known π^0 mass from the Σ^+ decay, while the three-momentum of the π^0 from the $\bar{\Sigma}^-$ is not required but treated as an unknown set of variables. This reduces the contamination from secondary showers induced by anti-protons annihilating in the EMC. If there is more than one π^0 candidate, that one with the smallest χ^2_{2C} is retained. A requirement on the quality of the 2C

kinematic fit of $\chi^2_C < 30$ is imposed to select the signal candidates.

The inclusive Monte Carlo (MC) samples of 10^{10} J/ψ events and 2.7×10^9 $\psi(3686)$ events are used to investigate possible sources of contamination. MC events passing the event selection are examined with TopoAna, a generic event-type analysis tool [50]. All particle decays are modeled with EVTGEN [51] using branching fractions either taken from the Particle Data Group (PDG) [49], when available, or otherwise estimated by MC simulations based on LUNDCHARM [52]. The main peaking background contributions are $\Psi \rightarrow \gamma \Sigma^+ \bar{\Sigma}^-$ and $\Psi \rightarrow \gamma \eta_c$ ($\eta_c \rightarrow \Sigma^+ \bar{\Sigma}^-$), with fractions estimated to be 0.1%. The main source of non-peaking background are the decays $\Psi \rightarrow \Delta^+ \bar{\Delta}^- \rightarrow p \pi^0 \bar{p} \pi^0$ and $\Psi \rightarrow p \pi^0 \bar{p} \pi^0$, which contribute 0.9% and 0.7% of the total data samples for J/ψ and $\psi(3686)$, respectively. Given the low level of peaking background, the sideband method is suitable for performing the background subtraction. Figure 2 shows the distribution of the invariant masses $M_{\bar{p}\pi^0}$ versus $M_{p\pi^0}$ from $\psi(3686)$ decays. The signal region in the green rectangle is defined as $1.167 < M_{\bar{p}\pi^0} < 1.212 \text{ GeV}/c^2$ and $1.172 < M_{p\pi^0} < 1.200 \text{ GeV}/c^2$. To determine the background contributions in the signal region, the sideband regions in the red rectangles are defined as $1.118 < M_{\bar{p}\pi^0} < 1.140 \text{ GeV}/c^2$, $1.240 < M_{\bar{p}\pi^0} < 1.262 \text{ GeV}/c^2$, and $1.172 < M_{p\pi^0} < 1.200 \text{ GeV}/c^2$. The mass windows are approximately $\pm 3\sigma$ away from the known $\bar{\Sigma}^-$ mass [49], with σ being the $M_{\bar{p}\pi^0}$ mass resolution. The background yields are estimated to be $f \times (B_1 + B_2)$, where B_1 and B_2 denote the number of background events in the rectangles, and $f = 1.06$ denotes the ratio of the background events between the signal and sideband regions determined by fitting the distribution of $M_{\bar{p}\pi^0}$. Here, the signal and background candidates are described by the signal MC shape and second-order polynomial function, respectively.

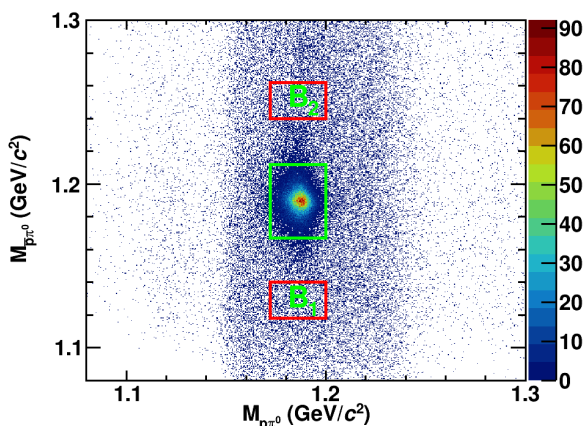


Figure 2. Distribution of $M_{\bar{p}\pi^0}$ versus $M_{p\pi^0}$ for the $\psi(3686)$ data sample. The variation in event density distribution is caused by the kinematic fit. The green box denotes the signal region, and the red ones indicate the sideband regions.

An unbinned maximum likelihood fit is performed with the five measured angles ξ as input. The fit is executed on the J/ψ and $\psi(3686)$ samples simultaneously and the free parameters are $\alpha_{J/\psi}$, $\alpha_{\psi(3686)}$, $\Delta\Phi_{J/\psi}$, $\Delta\Phi_{\psi(3686)}$, α_0 , and $\bar{\alpha}_0$. Following the approach in Ref. [19], the reconstruction efficiency is taken into account in a model-independent way and the background contribution is included with the scale factor f . The numerical fit results are summarized in Table I, where the derived values of $\langle\alpha_0\rangle$ and A_{CP} are also included. The relative phases between the Ψ electric and magnetic form factors are determined to be $\Delta\Phi_{J/\psi} = -0.2744 \pm 0.0033 \pm 0.0010$ rad and $\Delta\Phi_{\psi(3686)} = 0.427 \pm 0.022 \pm 0.003$ rad, respectively. This difference in sign indicates that the Σ^+ is polarized in such a way that its spins are aligned in opposite directions when produced via J/ψ decay compared to $\psi(3686)$ decay. This behavior was observed in an earlier BESIII study [20, 21] and is now confirmed with improved precision. The polarization can be studied graphically by defining the polarization estimator $M(\cos\theta_{\Sigma^+})$:

$$M(\cos\theta_{\Sigma^+}) = \frac{m}{N} \sum_i^{N(\cos\theta_{\Sigma^+})} (\sin\theta_p^i \sin\phi_p^i - \sin\theta_{\bar{p}}^i \sin\phi_{\bar{p}}^i), \quad (5)$$

where $m = 32$ is the number of bins, N is the total number of events in the data sample, and $N(\cos\theta_{\Sigma^+})$ is the number of events in the $\cos\theta_{\Sigma^+}$ bin. Figure 3 shows the Σ^+ polarization distributions where the opposite polarization directions for J/ψ and $\psi(3686)$ decays are evident.

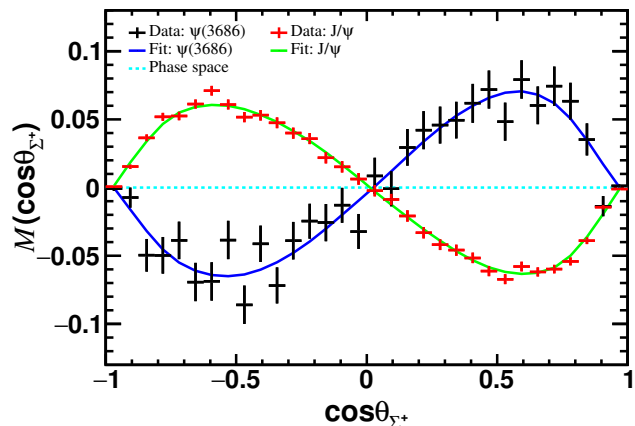


Figure 3. The moment $M(\cos\theta_{\Sigma^+})$ is a function of $\cos\theta_{\Sigma^+}$ for $\Psi \rightarrow \Sigma^+ \bar{\Sigma}^- \rightarrow p \pi^0 \bar{p} \pi^0$. The black and red data points with error bars are obtained independently via Eq. 5 for $\psi(3686)$ and J/ψ decays. The blue and green solid lines are drawn with the measured parameters, and the cyan dashed line represents the distribution without polarization uniformly distributed in phase space.

To investigate further the difference between J/ψ and $\psi(3686)$ decays, the quantity $R(\cos\theta_{\Sigma^+})$ is defined as the ratio of the polarization values (\vec{P}_h), measured according to Eq. 4, between $J/\psi \rightarrow \Sigma^+ \bar{\Sigma}^-$ and $\psi(3686) \rightarrow \Sigma^+ \bar{\Sigma}^-$ in

Table I. The decay parameters of $\Psi \rightarrow \Sigma^+\bar{\Sigma}^- \rightarrow p\pi^0\bar{p}\pi^0$ where the first uncertainty is statistical and the second systematic.

Parameter	This Letter	Previous result [21]
$\alpha_{J/\psi}$	$-0.5047 \pm 0.0018 \pm 0.0010$	$-0.508 \pm 0.006 \pm 0.004$
$\Delta\Phi_{J/\psi}$	$-0.2744 \pm 0.0033 \pm 0.0010$	$-0.270 \pm 0.012 \pm 0.009$
α_0	$-0.975 \pm 0.011 \pm 0.002$	$-0.998 \pm 0.037 \pm 0.009$
$\bar{\alpha}_0$	$0.999 \pm 0.011 \pm 0.004$	$0.990 \pm 0.037 \pm 0.011$
$\alpha_{\psi(3686)}$	$0.7133 \pm 0.0094 \pm 0.0065$	$0.682 \pm 0.030 \pm 0.011$
$\Delta\Phi_{\psi(3686)}$	$0.427 \pm 0.022 \pm 0.003$	$0.379 \pm 0.070 \pm 0.014$
$\langle\alpha_0\rangle$	$-0.9869 \pm 0.0011 \pm 0.0016$	$-0.994 \pm 0.004 \pm 0.002$
A_{CP}	$-0.0118 \pm 0.0083 \pm 0.0028$	$0.004 \pm 0.037 \pm 0.010$

each bin of $\cos\theta_{\Sigma^+}$ [40]. In Fig. 4, $R(\cos\theta_{\Sigma^+})$ is shown as a function of the Σ^+ scattering angle. $R(\cos\theta_{\Sigma^+})$ is negative over the full angular range, indicating that the sign of the polarization is opposite between the two decays in a given angular bin, consistent with the previous measurement of $\Psi \rightarrow \Sigma^0\bar{\Sigma}^0$ [53]. The larger sample size allows the magnitude of $R(\cos\theta_{\Sigma^+})$, which reflects the relationship between polarization differences in J/ψ and $\psi(3686)$ decays and the scattering angle, to be determined with interesting precision. It is found that the magnitude of $R(\cos\theta_{\Sigma^+})$ is smallest near $\cos\theta_{\Sigma^+} = \pm 1$, which corresponds to Σ^+ hyperons moving parallel (+) or antiparallel (-) to the positron beam. This is expected since at these angles, the production plane is not well-defined, and the polarization must therefore be zero. The magnitude of $R(\cos\theta_{\Sigma^+})$ increases at large angles, and reaches a maximum in the direction perpendicular to the beam axis.

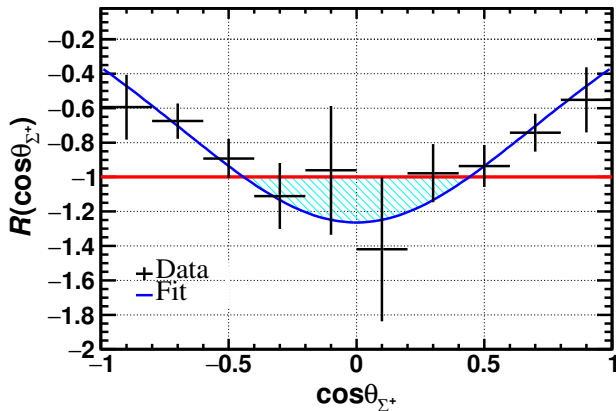


Figure 4. The angular distribution of the ratio of polarization between J/ψ and $\psi(3686)$ decays. The black dots with error bars are the data, the blue solid line is the fitting results, The red line represents a ratio of -1 . Comparing the Σ^+ from the J/ψ decay, the range of $\cos\theta_{\Sigma^+}$ in the shaded area (perpendicular to the electron beam direction) indicates the enhanced polarization of the Σ^+ in $\psi(3686)$ decays.

The systematic uncertainties are summarized in Table II where the totals are obtained from adding the individual components in quadrature.

The ratios of differences in efficiency between data

Table II. The uncertainties ($\times 10^{-3}$) of the parameters $\alpha_{J/\psi}$, $\Delta\Phi_{J/\psi}$, α_0 , $\bar{\alpha}_0$, $\alpha_{\psi(3686)}$, and $\Delta\Phi_{\psi(3686)}$. A dash (-) indicates that the uncertainties are negligible.

Source	$\alpha_{J/\psi}$	$\Delta\Phi_{J/\psi}$	α_0	$\bar{\alpha}_0$	$\alpha_{\psi(3686)}$	$\Delta\Phi_{\psi(3686)}$
Efficiency correction	0.1	0.3	0.7	0.9	0.2	0.3
Kinematic fit	0.6	-	-	-	1.9	2.1
Signal mass window	0.5	0.8	1.5	1.6	5.6	2.0
Background	0.3	0.3	-	-	2.4	-
Fitting method	0.6	0.3	0.6	3.6	1.4	0.1
Total	1.0	1.0	1.8	4.0	6.5	3.0

and MC simulation for charged-particle tracking, PID, and π^0 reconstruction are studied using the control samples $J/\psi \rightarrow p\bar{p}\pi^+\pi^-$ and $J/\psi \rightarrow \Sigma^+\bar{\Sigma}^- \rightarrow p\pi^0\bar{p}\pi^0$. The calculated ratios are then used as correction factors. Applying Gaussian sampling to the correction factors, and correcting samples with different factors, the phase-space MC sample is corrected 100 times and is used to determine the fit results. The uncertainty of the aforementioned ratios are taken as the width of the distribution of fit results. The average difference compared with the baseline result is taken as a systematic uncertainty. The uncertainty from the kinematic fit is estimated by varying the selection requirement of $\chi^2_{2C} \leq 30$ from 20 to 40. The uncertainty due to the requirement of signal mass window is determined by changing the window range. The uncertainty associated with the background subtraction is evaluated by varying the sideband window within a range of $4 \text{ MeV}/c^2$. We use the same criteria as for $\chi^2_{2C} \leq 30$ to quantify variations that cannot be explained by statistical fluctuations. The largest difference with respect to the baseline result is taken as a systematic uncertainty. To evaluate the reliability of parameter estimation with the maximum likelihood fit, a set of 100 MC samples is produced with EVTGEN and propagated through the BESIII detector. We use the angular distributions according to Eq. 3, with the parameter values obtained from the data analysis, and inspect the difference between input and output distributions. The difference is taken as the systematic uncertainty of the fitting method.

In summary, a five-dimensional angular analysis is simultaneously performed to the processes $J/\psi \rightarrow \Sigma^+\bar{\Sigma}^-$ and $\psi(3686) \rightarrow \Sigma^+\bar{\Sigma}^-$ selected from $(1.0087 \pm 0.0044) \times 10^{10}$ J/ψ events and $(2.7124 \pm 0.0143) \times 10^9$ $\psi(3686)$ events collected at the BESIII detector. Exploiting the quantum-entangled $\Sigma^+\bar{\Sigma}^-$ system and the self-analysing Σ decays, the measured precision of the parameters related to Σ pair production are improved by factors of three for $\alpha_{\psi(3686)}$, $\alpha_{J/\psi}$ and $\Delta\Phi_{\psi(3686)}$, and four for $\Delta\Phi_{J/\psi}$. The precision of the decay parameters α_0 and $\bar{\alpha}_0$ are improved by a factor of three and are consistent with the PDG average. The CP asymmetry, $A_{CP} = -0.0118 \pm 0.0083 \pm 0.0028$, is consistent with CP conservation within 1.3σ . The average value $\langle\alpha_0\rangle =$

$-0.9869 \pm 0.0011 \pm 0.0016$ is the most precise measurement in all baryon decays, and is a crucial input for precise decay parameter measurements and CP violation searches in the charm and beauty baryons decays to Σ^+ . Furthermore, it provides input for the observable measurements related to QGP in high-energy nuclear collisions. A detailed comparison of hyperon polarization with sign flip between J/ψ and $\psi(3686)$ decays are performed for the first time. Our measurements are expected to remain the most precise for Σ hyperons over the next decade, until results become available from future higher-luminosity machines [13, 16, 56].

The BESIII Collaboration thanks the staff of BEPCII and the IHEP computing center for their strong support. This work is supported in part by National Key R&D Program of China under Contracts Nos. 2023YFA1606000, 2020YFA0406300, 2020YFA0406400; National Natural Science Foundation of China (NSFC) under Contracts Nos. 12375070, 11635010, 11735014, 11935015, 11935016, 11935018, 12025502, 12035009, 12035013, 12061131003, 12192260, 12192261, 12192262, 12192263, 12192264, 12192265, 12221005, 12225509, 12235017, 12361141819; the Chinese Academy of Sciences (CAS) Large-Scale Scientific Facility Program; the CAS Center for Excellence in Particle Physics (CCEPP); Joint Large-Scale Scientific Facility Funds of the NSFC and CAS under Contract No. U1832207; CAS under Contract No. YSBR-101; 100 Talents Program of CAS; The Institute of Nuclear and Particle Physics (INPAC) and Shanghai Key Laboratory for Particle Physics and Cosmology; Agencia Nacional de Investigación y Desarrollo de Chile (ANID), Chile under Contract No. ANID PIA/APOYO AFB230003; German Research Foundation DFG under Contract No. FOR5327; Istituto Nazionale di Fisica Nucleare, Italy; Knut and Alice Wallenberg Foundation under Contracts Nos. 2021.0174, 2021.0299; Ministry of Development of Turkey under Contract No. DPT2006K-120470; National Research Foundation of Korea under Contract No. NRF-2022R1A2C1092335; National Science and Technology fund of Mongolia; National Science Research and Innovation Fund (NSRF) via the Program Management Unit for Human Resources & Institutional Development, Research and Innovation of Thailand under Contract No. B50G670107; Polish National Science Centre under Contract No. 2019/35/O/ST2/02907; Swedish Research Council under Contract No. 2019.04595; The Swedish Foundation for International Cooperation in Research and Higher Education under Contract No. CH2018-7756; U. S. Department of Energy under Contract No. DE-FG02-05ER41374.

[1] A. D. Sakharov, *Pisma Zh. Eksp. Teor. Fiz.* **5**, 32 (1967).

- [2] N. Cabibbo, *Phys. Rev. Lett.* **10**, 531-533 (1963).
- [3] M. Kobayashi and T. Maskawa, *Prog. Theor. Phys.* **49**, 652-657 (1973).
- [4] J. H. Christenson, J. W. Cronin, V. L. Fitch and R. Turlay, *Phys. Rev. Lett.* **13**, 138 (1964).
- [5] A. Abashian *et al.* (Belle Collaboration), *Phys. Rev. Lett.* **86**, 2509 (2001).
- [6] B. Aubert *et al.* (BaBar Collaboration), *Phys. Rev. Lett.* **86**, 2515 (2001).
- [7] Y. Chao *et al.* (Belle Collaboration), *Phys. Rev. Lett.* **93**, 191802 (2004).
- [8] B. Aubert *et al.* (BaBar Collaboration), *Phys. Rev. Lett.* **93**, 131801 (2004).
- [9] R. Aaij *et al.* (LHCb Collaboration), *Phys. Rev. Lett.* **122**, 211803 (2019).
- [10] R. Aaij *et al.* (LHCb Collaboration), *Phys. Rev. Lett.* **134**, 101802 (2025).
- [11] M. E. Peskin, *Nature* **419**, 24 (2002).
- [12] J. Tandean, *Phys. Rev. D* **69**, 076008 (2004).
- [13] N. Salone, P. Adlarson, V. Batozskaya, A. Kupsc, S. Leupold and J. Tandean, *Phys. Rev. D* **105**, 116022 (2022).
- [14] X. G. He, J. Tandean and G. Valencia, *Sci. Bull.* **67**, 1840-1843 (2022).
- [15] X. G. He, H. Murayama, S. Pakvasa and G. Valencia, *Phys. Rev. D* **61**, 071701 (2000).
- [16] E. Goudzovski, D. Redigolo, K. Tobioka, J. Zupan, G. Alonso-Álvarez, D. S. M. Alves, S. Bansal, M. Bauer, J. Brod and V. Chobanova *et al.* *Rept. Prog. Phys.* **86**, 016201 (2023).
- [17] T. D. Lee, J. Steinberger, G. Feinberg, P. K. Kabir and C. N. Yang, *Phys. Rev.* **106**, 1367 (1957).
- [18] M. Ablikim *et al.* (BESIII Collaboration), *Nature* **606**, 64-69 (2022).
- [19] M. Ablikim *et al.* (BESIII Collaboration), *Phys. Rev. Lett.* **129**, 131801 (2022).
- [20] M. Ablikim *et al.* (BESIII Collaboration), *Phys. Rev. Lett.* **131**, 191802 (2023).
- [21] M. Ablikim *et al.* (BESIII Collaboration), *Phys. Rev. Lett.* **125**, 052004 (2020).
- [22] J. F. Donoghue, X. G. He and S. Pakvasa, *Phys. Rev. D* **34**, 833 (1986).
- [23] J. Tandean and G. Valencia, *Phys. Rev. D* **67**, 056001 (2003).
- [24] M. Ablikim *et al.* (BESIII Collaboration), *Chin. Phys. C* **41**, 013001 (2017).
- [25] M. Ablikim *et al.* (BESIII Collaboration), *Chin. Phys. C* **42**, 023001 (2018).
- [26] J. M. Bickerton, R. Horsley, Y. Nakamura, H. Perlt, D. Pleiter, P. E. L. Rakow, G. Schierholz, H. Stüben, R. D. Young and J. M. Zanotti, *Phys. Rev. D* **100**, 114516 (2019).
- [27] B. Borasoy and B. R. Holstein, *Eur. Phys. J. C* **6**, 85-107 (1999).
- [28] A. Le Yaouanc, O. Pene, J. C. Raynal and L. Oliver, *Nucl. Phys. B* **149**, 321-342 (1979); H. G. Dosch, M. Jamin and B. Stech, *Z. Phys. C* **42**, 167 (1989).
- [29] M. Ablikim *et al.* (BESIII Collaboration), *Phys. Rev. D* **100**, 072004 (2019).
- [30] Y. B. Li *et al.* (Belle Collaboration), *Phys. Rev. Lett.* **127**, 121803 (2021).
- [31] L. K. Li *et al.* (Belle Collaboration), *Sci. Bull.* **68**, 583-592 (2023).

- [32] R. Aaij *et al.* (LHCb Collaboration), *Phys. Rev. D* **105**, L051104 (2022).
- [33] M. Burkardt and R. L. Jaffe, *Phys. Rev. Lett.* **70**, 2537-2540 (1993).
- [34] P. J. Mulders and R. D. Tangerman, *Nucl. Phys. B* **461**, 197-237 (1996).
- [35] M. Anselmino, D. Boer, U. D'Alesio and F. Murgia, *Phys. Rev. D* **63**, 054029 (2001).
- [36] F. Becattini and M. A. Lisa, *Ann. Rev. Nucl. Part. Sci.* **70**, 395-423 (2020).
- [37] F. Becattini, I. Karpenko, M. Lisa, I. Uppsala and S. Voloshin, *Phys. Rev. C* **95**, 054902 (2017).
- [38] L. Adamczyk *et al.* (STAR Collaboration), *Nature* **548**, 62-65 (2017).
- [39] Y. Guan *et al.* (Belle Collaboration), *Phys. Rev. Lett.* **122**, 042001 (2019).
- [40] G. Fäldt and A. Kupsc, *Phys. Lett. B* **772**, 16-20 (2017).
- [41] A. Z. Dubnickova, S. Dubnicka and M. P. Rekaló, *Nuovo Cim. A* **109**, 241-256 (1996).
- [42] G. I. Gakh and E. Tomasi-Gustafsson, *Nucl. Phys. A* **771**, 169-183 (2006).
- [43] G. Fäldt, *Eur. Phys. J. A* **51**, 74 (2015).
- [44] G. Fäldt, *Eur. Phys. J. A* **52**, 141 (2016).
- [45] M. Ablikim *et al.* (BESIII Collaboration), *Chin. Phys. C* **46**, 074001 (2022).
- [46] M. Ablikim *et al.* (BESIII Collaboration), *Chin. Phys. C* **48**, 093001 (2024).
- [47] M. Ablikim *et al.* (BESIII Collaboration), *Phys. Rev. D* **108**, L031106 (2023).
- [48] M. Ablikim *et al.* (BESIII Collaboration), *Nucl. Instrum. Meth. A* **614**, 345 (2010).
- [49] S. Navas *et al.* (Particle Data Group), *Phys. Rev. D* **110**, 030001 (2024).
- [50] X. Y. Zhou, S. X. Du, G. Li and C. P. Shen, *Comput. Phys. Commun.* **258**, 107540 (2021).
- [51] D. J. Lange, *Nucl. Instrum. Meth. A* **462**, 152 (2001); R. G. Ping, *Chin. Phys. C* **32**, 599 (2008).
- [52] J. C. Chen, G. S. Huang, X. R. Qi, D. H. Zhang and Y. S. Zhu, *Phys. Rev. D* **62**, 034003 (2000); R. L. Yang, R. G. Ping and H. Chen, *Chin. Phys. Lett.* **31**, 061301 (2014).
- [53] M. Ablikim *et al.* (BESIII Collaboration), *Phys. Rev. Lett.* **133**, 101902 (2024).
- [54] M. Ablikim *et al.* (BESIII Collaboration), *Phys. Rev. Lett.* **132**, no.8, 081904 (2024).
- [55] R. Barlow, [[arXiv:hep-ex/0207026](https://arxiv.org/abs/hep-ex/0207026) [hep-ex]].
- [56] M. Achasov, X. C. Ai, R. Aliberti, L. P. An, Q. An, X. Z. Bai, Y. Bai, O. Bakina, A. Barnyakov and V. Blinov *et al.* *Front. Phys. (Beijing)* **19**, 14701 (2024).